

**PRELIMBIC CORTEX INTEGRATES BEHAVIORAL CONTEXT WITH  
TASK-CODING DURING SPATIAL WORKING MEMORY MAINTENANCE**

by

John J. Stout Jr.

A thesis submitted to the Faculty of the University of Delaware in partial  
fulfillment of the requirements for the degree of Master of Science in Neuroscience

Spring 2018

© 2018 John J. Stout Jr.  
All Rights Reserved

**PRELIMBIC CORTEX INTEGRATES BEHAVIORAL CONTEXT WITH  
TASK-CODING DURING SPATIAL WORKING MEMORY MAINTENANCE**

by

John J. Stout Jr.

Approved: \_\_\_\_\_  
Amy L. Griffin, Ph.D.  
Professor in charge of thesis on behalf of the Advisory Committee

Approved: \_\_\_\_\_  
Robert F. Simons, Ph.D.  
Chair of the Department of Psychological and Brain Sciences

Approved: \_\_\_\_\_  
George Watson, Ph.D.  
Dean of the College of Arts and Sciences

Approved: \_\_\_\_\_  
Ann L. Ardis, Ph.D.  
Senior Vice Provost for Graduate and Professional Education

## **ACKNOWLEDGMENTS**

For the inspiration to pursue science, for countless opportunities that have been invaluable, and for mentoring me in a subject that I love dearly, I would like to thank Dr. Amy Griffin.

For teaching me the skills needed to complete this thesis and for being there every step of the way, I would like to thank Andrew Garcia.

Finally, without the support from my family and friends, the Griffin lab, my thesis committee, the individuals in the department of Psychological and Brain Sciences, and the OLAM staff, none of this could have been made possible. I will always be grateful for the support system that I have been a part of here at the University of Delaware.

## TABLE OF CONTENTS

LIST OF FIGURES .....	vi
ABSTRACT .....	ix
Chapter	
1 INTRODUCTION .....	1
1.1 Rodent mPFC and its Sub-Region, PL, is Functionally Implicated in SWM via Interregional and Intraregional Processes .....	1
1.2 ACC is Functionally Implicated in Motivation and Reward Expectancy .....	5
1.3 Aim of Study .....	7
2 METHODS .....	9
2.1 Subjects .....	9
2.2 Behavioral Apparatus .....	9
2.3 Handling, Pre-training, Training .....	10
2.4 Surgery Protocols .....	11
2.5 Perfusion and Histology .....	13
2.6 Recording and Cluster Cutting .....	14
2.7 Estimating Tetrode Locations for Individual Sessions .....	15
2.8 Medial Prefrontal Single Unit Firing Rate .....	16
2.9 Linear Classifier .....	17
2.10 Statistics .....	19
3 RESULTS .....	20
3.1 Histological Confirmation of PL and ACC Recordings .....	20
3.2 Task Phase-Selective Neurons in the mPFC .....	23
3.3 PL, but Not ACC Population Activity Discriminates Between the Late Portions of the Delay and ITI .....	26
3.4 PL Population Activity Distinguishes between Early and Late Start- box Occupancy .....	28
3.5 PL Distinguishes Between Distinct Experiences during the Beginning of the Delay .....	30
4 DISCUSSION .....	34
4.1 A Brief Summary of Our Findings .....	34
4.2 Task-Phase Analyses in the mPFC .....	35

4.3	PL Cortex Exhibits Differential Activity Between the Beginning and End of Start-box Occupancy .....	37
4.4	Prelimbic Population Activity Distinguishes Between Distinct Experiences .....	37
4.5	Conclusion.....	38
	REFERENCES .....	40
Appendix		
A	ANIMAL PROTOCOL PERMISSION .....	45

## LIST OF FIGURES

- Figure 1. - Histological confirmation of tetrode locations in the mPFC. **A)** Histological confirmation of final tetrode locations in the mPFC from two rats. **B)** Estimated locations of tetrodes for each session analyzed. **C)** Example clusters sorted (a total of 53 putative pyramidal cells) based upon waveform height, L-ratio, and isolation distance. ....21
- Figure 2. - A schematic of the DNMP task. There are two trial-types that are pseudo-randomly selected, one being a sample-left (sample L) traversal followed by a choice-right (choice R) traversal, or a sample-right (sample R) traversal followed by a choice-left (choice L) traversal. Each trial begins with a sample phase where the rat encodes the relevant trajectory and spatial environment while moving down the central stem, to a reward zone and back to the start box via the return arms where the rat is to maintain the previously encoded information for 20 seconds. After the delay, the rat enters the choice phase of the task where the previously encoded information is used to guide a decision at the choice point. If the animal traverses the arm opposite arm to the sample phase, then a rewarded is given. Finally, the rat enters the start-box for a 40 second inter-trial interval which precedes the next trial. ....22
- Figure 3. - Classification of task modulated prefrontal putative pyramidal cells (N = 53). **A)** Mean firing rate distribution. **B)** Percentages of significantly task modulated units ( $p < 0.05$ , Wilcoxon Signed Rank Test). A total of 53.3% of all mPFC units recorded were significantly task phase modulated. Of all units recorded, 23.3% were significantly task phase modulated by the last 5 seconds of start-box occupancy (late start-box task phase modulated in **green**), 3.3% were significantly task phase modulated by the first 5 seconds of start-box occupancy (early start-box task phase modulated in **orange**), 10% were significantly modulated by task phase during stem traversals (stem task phase modulated in **grey**), and 16.7% were significantly modulated by task phase during choice point occupancy (choice point task phase modulated in **yellow**). **C)** example unit from the last 5 seconds of start-box occupancy – notice the difference in firing rate between the delay and ITI (red arrow). ....25

Figure 4. - PL, but not ACC population distinguishes between the late delay (last 5 seconds of the delay) and late ITI (last 5 seconds of the ITI). A Linear Classifier was trained to distinguish between task phases (i.e. delay vs ITI, sample stem vs choice stem). The right-most sub-panels for **A** and **B** depicts linear classifier output when trained to distinguish between early delay and ITI (referred to as Early), and trained to distinguish between late delay and ITI (referred to as Late) **A**) Linear classifier trained on all recorded units (N = 53) **B**) Linear classifier trained on PL (N = 30) and ACC (N = 23). PL population activity is predictive of whether the animal is in the late delay or late ITI task phases ( $p < 0.01$  one-sample  $t$ -test) and predicts late start-box occupancy significantly better than ACC ( $p < 0.01$  two-sample  $t$ -test assuming unequal variance) \* indicates  $p < 0.05$ ; \*\* indicates  $p < 0.01$ . .....27

Figure 5. - PL distinguishes between early and late start-box occupancy. **A**) Upper panel is an example showing the firing rate of a unit during the delay. Lower panel depicts a linear classifier trained to distinguish between the early and late delay. PL but not ACC population activity distinguishes between the early and late delay at a level significantly above chance (PL  $p < 0.01$  one-sample  $t$ -test; ACC  $p > 0.05$  one-sample  $t$ -test). **B**) Upper panel is an example showing the firing rate of a unit during the ITI. The lower panel depicts a linear classifier trained to distinguish between the early (first 5 seconds) and late (last 5 seconds) ITI. PL distinguishes significantly above chance ( $p < 0.001$  one sample  $t$ -test), ACC distinguishes significantly above chance ( $p < 0.05$  one sample  $t$ -test) and PL better distinguishes between early and late ITI ( $p < 0.05$  two sample  $t$ -test assuming unequal variances). \* indicates  $p < 0.05$ ; \*\* indicates  $p < 0.01$ ; \*\*\* indicates  $p < 0.001$ . .....29

Figure 6. - PL population distinguishes between trial-type during early delay. **A)** Depiction of the different trial-types on the DNMP task. **B)** PL population activity (N = 30) does not distinguish between trial-types when the classifier is trained on activity during the entire delay ( $p > 0.05$  one-sample *t*-test). **C and D)** A linear classifier was trained to distinguish between trial-types during the early and late delay. **C)** Due to an unequal number of trial-types, one trial was randomly removed. PL ensemble can accurately predict the trial-types in the early delay ( $p < 0.05$  one-sample *t*-test); prediction is significantly better than during the late delay ( $p < 0.01$  two-sample *t*-test assuming unequal variances). **D)** Averaged linear classifier accuracy when each trial was removed separately. PL can accurately distinguish between trial-types during the early delay ( $p < 0.05$  one-sample *t*-test) and significantly greater than during the late delay ( $p < 0.001$  two-sample *t*-test assuming unequal variances). \* indicates  $p < 0.05$ ; \*\* indicates  $p < 0.01$ ; \*\*\* indicates  $p < 0.001$ . .....32

Figure 7. - PL distinguishes between trial-type in the early delay, but not significantly above chance during the early ITI. **A)** Schematic of the analysis. **B)** A linear classifier was trained to discriminate between trial-types in the early delay and early ITI. Random deletion of trials within trial-types was utilized due to unequal number of trials between trial-types (see methods). PL distinguishes between trial-types in the early delay significantly greater than chance ( $p < 0.05$  one-sample *t*-test) and significantly greater than during the early ITI ( $p < 0.05$  two-sample *t*-test assuming unequal variances). PL does not distinguish trial-types significantly above chance during the early ITI ( $p > 0.05$  one-sample *t*-test). **C)** Averaged linear classifier percent accuracy. Trials were randomly excluded from the analysis for a total of 12 times (see methods). Linear classifier accuracy is significantly greater in the delay than the ITI ( $p < 0.001$  two-sample *t*-test assuming unequal variances), and significantly greater than chance for early delay ( $p < 0.05$  one-sample *t*-test), but not for early ITI ( $p > 0.05$  one-sample *t*-test). \* indicates  $p < 0.05$ ; \*\*\* indicates  $p < 0.001$ . .....33

## ABSTRACT

Spatial working memory (SWM) is the ability to hold information on-line for future use. Numerous studies have investigated the prefrontal mechanisms that support SWM processes, but it is not fully understood what spatially relevant representations are supported during memory maintenance. Using *in vivo* electrophysiological recordings from rodent prelimbic (PL) and anterior cingulate cortices (ACC) (two sub-regions of the medial prefrontal cortex that have dissociable functional roles in behavior), we have replicated the finding that the mPFC exhibits firing rate related changes that may be related to maintenance processes. In line with previous work examining mPFC activity, we demonstrate that PL cortex population activity discriminates between the end of the delay and inter-trial interval, suggesting that PL plays a role in task-coding. Furthermore, PL cortex discriminates between the early and late portions of the delay, and the early and late portions of the ITI, possibly reflecting preparatory processes. Finally, we are the first to our knowledge to report that PL cortex firing rate distinguishes between trial-types (sample L-choice R vs sample R-choice L) on the delayed non-match to position task during the early, but not late delay period. These findings suggest that PL cortex integrates task-coding and behavioral context during SWM maintenance.

## Chapter 1

### INTRODUCTION

#### **1.1 Rodent mPFC and its Sub-Region, PL, is Functionally Implicated in SWM via Interregional and Intraregional Processes**

Spatial working memory (SWM), or the ability to hold spatial information in “mind” for an epoch, depends on the medial prefrontal cortex (mPFC), hippocampus (HC), and mPFC-HC interactions (Floresco et al., 1997; Lee & Kesner 2003; Churchwell & Kesner 2011; Hallock et al., 2016; see Griffin et al., 2015 for a review). Studies have demonstrated that mPFC lesions disrupt SWM on a variety of SWM tasks (Floresco et al., 1997; Wang & Cai 2006; Lee & Kesner 2003; Churchwell & Kesner 2011). Interestingly, lesions restricted to the prelimbic (PL) and infralimbic (IL) sub-regions, but not the anterior cingulate cortex (ACC) sub-region impairs performance on both the delayed-alternation (DA) and delayed non-match to position (DNMP) tasks (Neave et al., 1994; Ragozzino et al., 1998; Sánchez-Santed et al., 1997; see Kesner & Churchwell, 2011 for a review).

The fundamental difference between the DA and DNMP task is that the DNMP task can be separated into distinct task phases (cue-based encoding during the sample phase, memory maintenance during the delay phase, and memory-guided decision making during the choice phase). This parcellation of the task provides the

means to investigate the neuronal mechanisms supporting the encoding, maintenance, and retrieval of SWM.

For almost 50 years, studies have alluded to the ‘working memory engram’ as elevated, sustained neuronal firing rates for goal-relevant information during the delay period (Fuster, 1971; see Goldman-Rakic 1995 for review). Although sustained firing rates have not been extensively observed in the rodent during memory maintenance, multiple groups have observed delay-related phenomena within the prefrontal cortex such as increased theta power (Myroshnychenko et al., 2017), prefrontal-hippocampal theta synchrony (Myroshnychenko et al., 2017), prefrontal-thalamic synchronous activity (Bolkan et al., 2017), and elevated firing rates during the delay preceding a goal (Jung et al., 1998; Yang et al., 2014; Bolkan et al., 2017).

With regards to elevated firing rates during the delay, Yang et al., (2014) discovered that single units can differentially fire during the beginning, middle, or end of the delay period. In support of these findings, Jung et al., (1998) showed that the mPFC exhibits a wide variety of firing rate correlates on spatial working memory tasks, including goal-relevant delay-specific firing. While the studies mentioned above focused on single unit correlates, there are reports of population activity correlates during the delay. For example, a recent study showed that neuronal population firing patterns during the delay period (on a two-alternative forced choice task) reflect information about which rule is currently relevant for goal-oriented decision making (Schmitt et al., 2017). Another study demonstrated that mouse mPFC population activity is capable of distinguishing between task-phase (sample or choice), on a

DNMP task prior to entering the stem, reflecting mPFC population task-coding during start-box occupancy (Spellman et al., 2015). These studies demonstrate that the mPFC can exhibit spatial tuning and support the possibility that the mPFC is maintaining goal directed-spatially relevant information and/or rules.

While sustained prefrontal activity alone, during a delay period, is not a common finding in rodent literature, recent work from Bolkan et al., (2017) found that projections from the medial dorsal thalamus (MD) support the ability of the mPFC to maintain previously encoded information. In this study, maintenance activity was represented by elevated, and tiled neuronal activity (whereby some groups of neurons fire in the beginning of the delay and as they decrease in firing, other groups simultaneously increase their firing) during the DNMP task. Interestingly, delay-elevated units didn't increase their firing rates when the rat made an error, or with optogenetic suppression of MD-mPFC terminals. Furthermore, this tiled population activity could support changes in neuronal representations during memory maintenance, like a shift in retrospective to prospective activity states (Ito et al., 2015; Myroshnychenko et al., 2017; Kesner, 1989).

Retrospective and prospective memory representations are operationally defined here as neuronal activity that is reflective of a previous or future experience, respectively (Cook et al., 1985; Kesner, 1989; Ito et al., 2015; Myroshnychenko et al., 2017). It has been suggested for decades that the brain utilizes retrospective and prospective codes to make decisions (Cook et al., 1985; Kesner, 1989). Cook et al., (1985) devised a spatial delayed alternation task, using a 12-arm radial maze, and

imposed a 15-minute delay prior to the 2<sup>nd</sup>, 4<sup>th</sup>, 6<sup>th</sup>, 8<sup>th</sup>, or 10<sup>th</sup> choice in separate sessions. They found that imposing a delay in the middle of the choice sequence had the largest effect on choice accuracy, but imposing the delay in the beginning or at the end of the sequence had less of an effect on behavior. These findings suggest the use of retrospective information in the early sequences, but prospective memory in the later sequences. In line with these findings, Kesner, (1986) inactivated the mPFC with aspiration lesions and discovered that rats with prefrontal lesions make more errors during the later sequences, suggesting that the mPFC shifts from a retrospective to a prospective memory representation.

In support of these behavioral manipulations, Myroshnychenko et al., (2017) set out to determine if the pathway from the hippocampus to the mPFC supports retrospective memories, and if the prefrontal cortex shifts to a prospective representation for a future choice, as was suggested above. Recording single units in the mPFC and local field potentials (LFP) in mPFC and HC, Myroshnychenko et al., (2017) utilized a delayed spatial win-shift task and discovered that as the delay period progressed, mPFC single units became more entrained to hippocampal theta and mPFC ensemble activation patterns shift from most closely representing a previous experience (the activation pattern during the training trial on the delayed spatial win-shift task) to most closely matching a future one (the activation pattern on the subsequent testing trial). Furthermore, other groups have also focused on how prefrontal delay-period firing rates represent experiences throughout a delay (Baeg et al., 2003; Ito et al., 2015). In fact, Baeg et al., (2003) found that neuronal activity from

the same set of cells during the delay period of a DA task represents past and future goal arm choices. While Ito et al., (2015) showed that delay activity can not only represent a retrospective experience, but that prefrontal activity during the delay is also predictive of future choice and error trials on a DA task. Collectively, these studies demonstrate that the rodent mPFC ensembles shift from a retrospective to prospective memory representation during the maintenance period of spatial working memory.

## **1.2 ACC is Functionally Implicated in Motivation and Reward Expectancy**

The studies mentioned above highlight the role of the PL in spatial working memory; however, in contrast to PL cortex, the rodent ACC cortex is thought to be implicated in motivational aspects of choice-related behavior (Walton et al., 2002; Walton et al., 2003; Hillman & Bilkey 2010), in reward expectancy, and prediction errors (Hyman et al., 2017). In fact, Walton et al., (2003) used a high-cost/high-reward task in which rats learned that if they climbed over a barrier (high-cost) they would receive a greater reward. When the ACC was lesioned excitotoxically, rat behavior transitioned from consistently choosing the high-cost/high-reward response to a low-cost/low-reward response, suggesting that the ACC is involved in motivational aspects of choice-related behavior. In support of this, Hillman & Bilkey (2010) demonstrated that many units prefer to fire during the high-cost/high-reward goal traversals and discovered that devaluing the high-cost/high-reward traversals to high-cost/low-

reward traversals corresponds with units firing more towards the low-cost trajectory. Together these findings suggest that ACC is critical for cost-benefit analyses.

As mentioned above, ACC is also involved in reward expectancy. Hyman et al., (2017) utilized a probabilistic selection task in rodents whereby animals chose one of three nose-poke holes to receive a reward; however, the likelihood of receiving a reward is different for each hole. To elaborate, there was a 75% chance of receiving a reward from one hole, a 50% chance of receiving a reward from another hole, and a 25% chance of receiving a reward from the final hole. While the animal was performing the task, the experimenters switched the probabilities of receiving a reward between the 75% chance hole and 25% chance hole. They found that the ACC exhibited expectancy-related neuronal activity. Specifically, the neuronal population exhibited a change in firing rate that accompanied a behavioral modification suggesting that the rat adapted to the new set of probabilities. They also found that the population activity in the ACC represents a prediction error, or a situation where not receiving an expected reward is represented in the ACC ensemble activity. To elaborate, first the authors found that the ensemble of cells is predictive of whether the animal will or will not receive a reward. Next, they demonstrated that if the animal received a reward on multiple trials, the ACC ensemble would continue to more closely match trials where the animal received a reward; however, if the animal did not receive a reward, the population would quickly shift to be representative of the no-reward state. These results suggest that the ACC not only exhibits expectancy related signaling, but also represents prediction error. Interestingly, the studies above could

support ACC being involved in SWM because animals are rewarded after a correct decision. However, Ragozzino et al., (1998) demonstrated that lesioning of the dorsal ACC did not affect behavioral accuracy on a 12-armed SWM task. While this finding suggests that the rodent ACC is not implicated in SWM, the studies mentioned above could support the ACC being involved in processes that guide learning.

### **1.3 Aim of Study**

While the studies mentioned above demonstrate the importance of the PL cortex in SWM, it is still not fully understood what spatially-relevant representations are supported by the PL cortex during memory maintenance on the DNMP task. Since the ACC is not implicated in SWM, we used it to contrast PL cortex activity to explore the neuronal representations that the PL cortex may support during the maintenance period on a DNMP task.

First, we predicted that we would see delay-elevated and start-box discriminative firing rates in the mPFC analogous to the studies mentioned above. Next, utilizing a linear classifier trained on firing rates, we predicted that the mPFC population activity would be discriminative between the delay and inter-trial interval (ITI) like seen in Spellman et al., (2015) in mice, and between the sample and choice. After separating PL and ACC neurons, we predicted that PL sub-region population activity would distinguish between the delay and ITI, and between task-phases. Further, since the ACC is not implicated in SWM performance, we predicted that we

would not see discriminating population activity between the start-box task-phases (delay and ITI) and between task-phases. We also wanted to determine if the PL cortex distinguishes between the early and late portions of the delay period (first 5 and last 5 seconds, respectively) of the DNMP task. Finally, we wanted to determine if the PL could distinguish between discrete trial-types (sample-left/choice-right vs sample-right/choice-left) during the delay period, which would suggest that the PL cortex supports two separate neuronal representations during the DNMP task and that maintaining the correct representation is related to SWM performance.

## **Chapter 2**

### **METHODS**

For complete disclosure, the rats in this study were used for multiple experiments, but only the data from the study proposed in the introduction will be reported for purposes related to the defense of this thesis. Any procedures that occur post-mortem and are not used for this experiment will not be mentioned in this proposal. Both rats were injected with channelrhodopsin-2 (ChR2) in the mPFC, but one was also injected with archaerhodopsin-T009 (ArchT) in the Re. The procedures related to the injected adeno-associated viruses (AAV) will not be mentioned in depth further.

#### **2.1 Subjects**

Both subjects were adult (>90 days) Long Evans rats (ordered from Harlan, IN). The subjects were kept on a food restriction of 4-5 pellets per day to maintain 90% of their *ad libitum* body weight. The colony room was temperature and humidity controlled with a 12-hour light on-light off cycle with experimentation occurring during the light-on period.

#### **2.2 Behavioral Apparatus**

The behavioral apparatus was a modified wooden T-maze painted black. The maze consisted of a stem (116 x 10 cm), two goal arms (56.5 x 10 cm), and two return

arms (112 x 10 cm), which were surrounded by a 6 cm tall wooden wall. At the base of the maze, there was a pedestal (a ceramic bowl glued to a barstool) where the rat waited between trials (ITIs) and during a delay within trials (delay periods), where they were blocked from maze entry by a wooden barricade. The maze was surrounded by black curtains with large visual cues and located in a room dimly lit by a compact fluorescent light bulb.

### **2.3 Handling, Pre-training, Training**

Rats were handled for 5 days prior to being put on the maze. After handling, rats were placed in each goal arm for three minutes (goal box training) with baited cups of sprinkles. If the rats ate the sprinkles within ninety seconds, the trial was considered correct. After one day of eating the sprinkles within ninety seconds for 6 consecutive trials, rats began the next phase of training: forced runs. During forced runs, and starting at the pedestal, rats were forced to choose one of the goal arms, eat 2-3 sprinkles that were in a bottle cap attached with Velcro to the maze, then return to the pedestal. Forced runs consisted of an equal number left and right traversals of the maze for twelve trials in total. When subjects ate on all trials, and maze behavior was adequate (entering the stem, no signs of fear-like freezing) they began the task-training phase. During task-training for the DNMP task, rats began at the pedestal. The barricade was lifted, allowing the rats to enter the stem. The first traversal, or the sample phase of the task, is analogous to the forced runs previously mentioned. After

moving through each choice point, rats entered the goal arms to receive their reward, traverse the return arm, then wait in the pedestal for a delay period of approximately 20 seconds. Following the 20 second delay, the barricade was lifted, and they entered the stem. After traversing the stem, the rats were rewarded with 2-3 sprinkles for traversing the goal arm that was not previously visited. Criterion is met when rats reach greater than or equal to 80% for two consecutive days, or when the rat reaches 100% for one day (Figure 2).

## **2.4 Surgery Protocols**

Animals were first injected with AAV vectors in a separate surgery. Then, a second surgery took place after rats reached asymptotic levels of choice accuracy on the DNMP task. Rats experienced the same protocol mentioned above, up and until the marking of the skull with the burr. For the mPFC craniotomy, a burr hole was made over the left hemisphere using 3.25 mm anterior and 1.15 mm lateral to bregma. Next, using a 0.007 mm diameter burr, a mark was made in the skull (over the right hemisphere) at 2.3 mm posterior to bregma and 2.0 mm lateral to bregma for the Re craniotomy. Afterwards, using a 0.007mm diameter burr, a hole was made over the left hemisphere hippocampus at 4.2mm posterior to bregma, 2.4mm lateral to the sagittal sinus and 2.1 mm ventral to dura. After the burr holes were made, another four burr holes were made using the 0.007 mm diameter burr for four small bone screws (Fine Science Tools) placements, further referred to as “anchor screws.” A final burr

hole using the 0.009 mm diameter burr was made over the cerebellum for placement of the ground wire. Next, a trephine was attached to the drill, the burr hole centers lined up with the center of the trephine, and craniotomies were made. For the mPFC, the previous craniotomies, if healed, were removed with either forceps, trephine, or a combination. The new craniotomy over the mPFC was made using a larger diameter trephine (3 mm diameter), centered around the burr hole. Four stainless steel wires (A-M Systems) were placed into hippocampus for local field potential recordings (LFP), using the coordinates mentioned above but lowered 2.1mm ventral to bregma, and stabilized using dental acrylic. The Re fiber (FG200UEA, THORLABS) glued inside a 1.25 mm Ceramic Stick Ferrule (THORLABS) was then cemented to two stainless steel wires (A-M Systems) for LFP recordings and encased in a 21g cannula (Component Supply Co.) and was slowly lowered into the right hemisphere at a 15° angle 7.25 mm ventral to dura, using the same coordinates mentioned above for Re virus injection and stabilized using dental acrylic. The Microdrive (see Image under this section) was placed slightly into the left hemisphere mPFC at a 7° angle, centered with the larger craniotomy hole (coordinates mentioned above for mPFC drive placement). When in place, GLUture was added to the craniotomy with the bundle, and dental acrylic cemented the drive to the skull. After the first layer of dental acrylic is added, the ground wire was attached via a 30g cannula, to a corresponding wire attached to the electrode interface board (EIB, Neuralynx). The rat was given an injection of Flunixin (Banamine; 2.5 mg/kg) while placing the second coat of acrylic

to cement the drive with the fiber. Children's ibuprofen (30 mg/kg) was be given to the rats for 2-4 days; the rats also received oral antibiotics in their water.

## **2.5 Perfusion and Histology**

Electrolytic lesions were made by passing 11.9  $\mu$ A of current through one wire of each tetrode, and through the reference wire. After a 24-hour period, rats were anesthetized, and an injection of sodium pentobarbital was given. When a drastic slowing of the rats breathing was observed in combination with a paw pinch to ensure no reflexive response, the rats were transcardially perfused. The first rat was perfused with PBS and Formalin, but the second was perfused with TBS and 4% paraformaldehyde (PFA). A guillotine will be used for decapitation, some skull was removed from the back of the head to reveal the cerebellum, and the head soaked in 4% PFA for 1-3 days. Next, the tetrodes were raised from the brain, the brain was extracted and placed in a 9% sucrose solution and allowed to sit until it dropped to the bottom of the scintillation vial. The brains were frozen in the cryostat prior to sectioning.

For cresyl-violet staining, slides were first dipped in distilled water. Next, slides were immersed in the following concentrations of EtOH for 2 minutes each; 100% EtOH, 95% EtOH, 70% EtOH, and 50% EtOH. They were dipped in distilled water and allowed to sit in cresyl-violet stain until slides were dark. Next slides were placed in distilled water for 1 minute, then placed in the following concentrations of

EtOH for 3 minutes; 50% EtOH, 70% EtOH, 95% EtOH, 100% EtOH, then in a separate 100% EtOH container. Slides were placed in xylene for 5 minutes, then allowed to sit until cover slipped. Toulene was placed on the slides prior to the cover slip, and the slides sat out to dry when finished.

Immunohistochemical (IHC) staining was used for a separate experiment with optogenetics; however, this thesis used mPFC slices that underwent the IHC staining procedure. First, slides were first washed 3 times with 1X Tris-Buffered Saline (TBS) for 5 minutes each. Once slides were dry, a PAP pen was used to line the edges of the slides. A stock solution made of 1X TBS, Normal Goat Serum (NGS), and Digitonin was utilized and 3 drops were applied to each slide (1 vial contained 950uL 1X TBS, 50uL NGS, and 2uL Digitonin). Following a 1 hour incubation period, the stock solution was added to the slides again with the addition of an antibody (2uL antibody added to the stock solution). After a 24hr incubation period, slides were washed, the secondary antibody was added and the slides incubated for 1 hour. Finally, slides were washed, and two drops of ProLong Diamond Antifade Mountant were added to each slide and cover-slipped.

## **2.6 Recording and Cluster Cutting**

Prior to the animal performing the task, tetrodes were lowered into the brain and given 30 minutes - 1 hour to settle. Neural activity was recorded for 10-20

minutes prior to recording and after recording. Recording sessions included in this thesis took place on days when optogenetic testing did not occur.

Recordings were acquired using a Digital Lynx (Neuralynx) 64-channel recording system. Using a mounted ceiling video camera and a video tracker, rat position was tracked based on LED illumination. Cheetah (Neuralynx) was used for acquisition and recording of spikes from single units and for continuously sampled LFP. Single unit spiking was sampled at 32 kHz and band-pass filtered between 0.6 – 6 kHz, with a spike waveform amplitude of between 50 and 75  $\mu\text{V}$  being used as the threshold (this largely varied depending on the tetrodes). Spike clusters were identified visually, plotted using Spikesort 3D (Neuralynx), cut using *Klustakwik*, and manually sorted based on spike waveform height, peak amplitude, and if L-ratio (a measurement used to determine the quality of a cluster based on how separate the spikes are between clusters) value is  $<0.1$  (Schmitzer-Torbert et al., 2005). Putative pyramidal cells and putative interneurons were separated based on spike waveform width and firing-rate, with only putative pyramidal cells being included for analyses (Figure 1C).

## **2.7 Estimating Tetrode Locations for Individual Sessions**

Tetrode location for each session was accomplished by first determining the final location of the tetrode (this was achieved by first overlaying a brain atlas slices from Paxinos & Watson, 1986 over the imaged brain slices and localizing the electrolytic lesion mark). Next the putative tetrode was identified by considering the

location of the tetrode in the bundle and the bundle length and width. Using multiple final lesion locations, multiple brain slices, and a turn count sheet with every recorded turn, the putative tetrodes along with their depths were identified. Next, using a recorded turn count sheet, we calculated the locations of the tetrodes for each session (Figure 1B; grey dots represent tetrode locations).

## **2.8 Medial Prefrontal Single Unit Firing Rate**

Single-unit firing rate on the maze was quantified by dividing the number of spikes emitted by time. For example, during the delay period, quantifying the last 5 seconds of the delay was achieved by finding the time point at which the delay ended, subtracting 5 seconds, finding the total number of spikes within that time window and dividing the number of spikes by 5 seconds (Figure 3 shows distribution of cell firing rates). The mean firing rate for each neuron was determined by extracting the time at which the task began and ended, finding the total length of time in between, extracting the spikes recorded and dividing by the total amount of time (Figure 3A). The peri-stimulus time histogram depicted in Figure 3C was smoothed with Gaussian filtering and used to visualize the raster plot above it.

Task phase selective firing was determined by calculating firing rates at the startbox, stem, and choice point for both the sample and choice task phases, then using a Wilcoxon Signed-Rank test to determine if the firing rate was significantly different between two observations (i.e. firing rate on the stem during sample phase vs firing

rate on the stem during the choice phase, or firing rate during the last 5 seconds of the delay vs firing rate during the last 5 seconds of the ITI).

## 2.9 Linear Classifier

A linear classifier was utilized to determine if the mPFC populations exhibit unique patterns of activity that distinguish between two classes of choice (i.e. sample task phase vs choice task phase); the same linear classifier was used in Hallock et al., (2016), however this thesis utilized a pseudo-simultaneous method. To elaborate, instead of running the linear classifier on each session and averaging the values, we included all cells firing rates even though they were not all recorded in the same session (see Spellman et al., 2015 for a similar approach). For all linear classifier analyses, only “good” sessions (80% or higher performance) were included. The linear classifier utilizes a method where it is trained on all trials but one, then tested on the one left out; it repeats this for all the trials.

A linear classifier can solve an optimization problem (the problem finding the best solution of all possible solutions) based on the training data from the following:

$$\arg \min R(w) + C \sum_{i=1}^N L(y_i, w^T x_i)$$

where  $R(w)$  prevents overfitting,  $w$  sets the classifier parameters,  $C = I$  as a penalty parameter for misclassification, and  $L(y_i, w^T x_i)$  allows for an estimation of the difference between the prediction made by the classifier and the true output from the

training example. To elaborate further, the linear classifier is capable of taking firing rate training data and plotting an optimal hyperplane based on the maximum margins dictated by the data. The output of the classifier is defined by the following equation:

$$y = f(\vec{w} \cdot \vec{x}) = f\left(\sum_j w_j x_j\right)$$

where  $y$  is the output score,  $f$  assigns a binary variable (1, -1) used for classification of classes of interest,  $\vec{w}$  being the vector of weights learned from the training samples, and  $\vec{x}$  will be the mean firing rates. The output value is then compared with its testing label (1,-1) and decoding accuracy is defined as the number of correctly identified classes (i.e. sample vs choice, early delay vs late delay, trial-type sample L-choice R vs trial-type sample R-choice L) divided by the total number of labels.

For mPFC classification of task phase, the linear classifier was trained on bins of firing rate matrices, and the classifier was to determine if the population vector of firing rates most closely matched the sample or choice task phase (for the startbox, the classifier was trained to distinguished between delay and ITI). For mPFC classification of the early (first 5 seconds) vs late (last 5 seconds) delay, only correct trials were considered.

For trial-type linear classification, only correct trials were considered. Further, because some sessions include both cells from behavioral performance of 83.4% and 88.9%, the amount of trial-types differed. To compensate and to ensure that the linear classifier was trained on an equal number of trial-types, we opted to randomly eliminate one trial in the data set from Figure 6D. To calculate the Averaged Linear

Classifier Accuracy in Figure 6E, we eliminated each trial, ran the linear classifier, and averaged all of the average performances without each trial. For the early ITI data-set in Figure 7, two trials had to be eliminated. Further, for the early delay data-set in Figure 7B and 7C, two trials from one trial-type and one trial from the other trial-type had to be eliminated to match the number of trial-types in the early ITI. To determine if our findings were being driven by random elimination, we opted to randomly eliminate trials for a total of 12 times and average our findings (Figure 7C). We decided to use 12 random eliminations because it provides the same statistical power as in Figure 7B.

## **2.10 Statistics**

For classification of task phase modulated units, Wilcoxon Signed-Rank test was utilized due to firing rate being a nonparametric variable. To determine if linear classifier performance was significantly greater than chance, a one-sample *t*-test was utilized. A two-sample *t*-test assuming unequal variances was used to determine if one groups linear classifier percent accuracy was significantly greater than the other. Findings were considered reliable if the  $p < 0.05$ .

## **Chapter 3**

### **RESULTS**

#### **3.1 Histological Confirmation of PL and ACC Recordings**

First, we confirmed mPFC tetrode placement via histological procedures mentioned in the methods section. The upper panel of Figure 1A shows a representative coronal section stained with cresyl-violet showing a thermoelectric lesion in the mPFC, while the lower panel shows the same except stained using an IHC protocol. For each included session, tetrode locations were estimated (see methods for more information) and these estimations were used to sort clusters as belonging to either PL or ACC. A total of 10 tetrodes in PL and 8 tetrodes in ACC were used to record neurons. Of the 8 tetrodes in ACC, 3 were also used to record from PL. Only putative pyramidal cells were included for analyses in this thesis (Figure 1C; see methods).

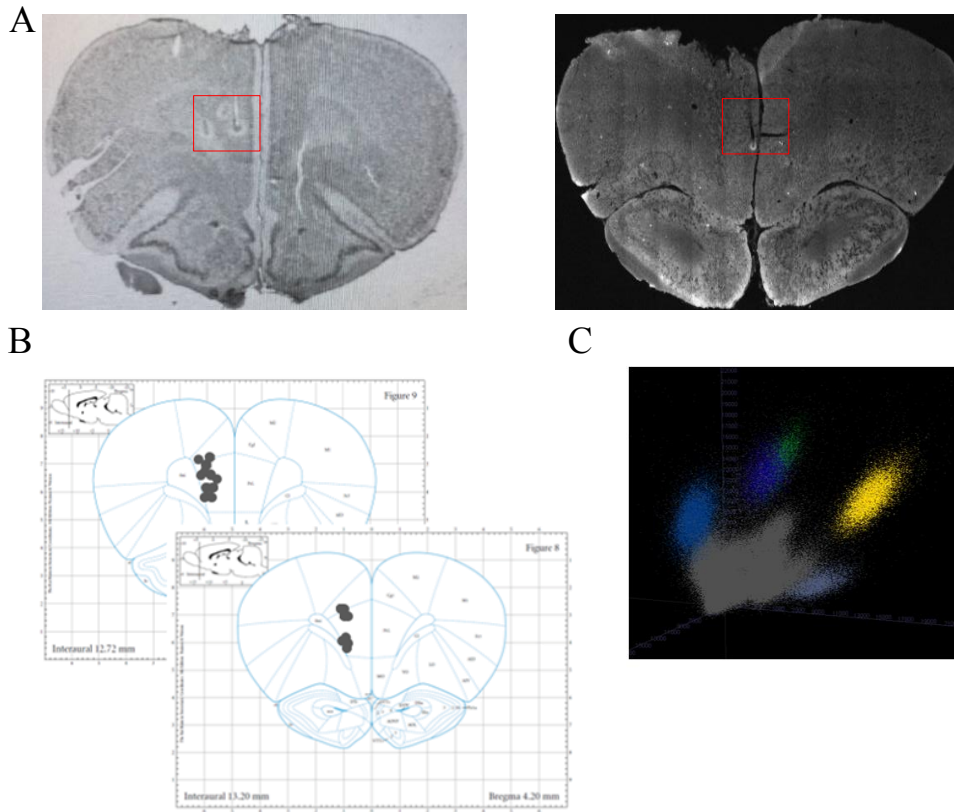


Figure 1: Histological confirmation of tetrode locations in the mPFC. **A)** Histological confirmation of final tetrode locations in the mPFC from two rats. **B)** Estimated locations of tetrodes for each session analyzed. **C)** Example clusters sorted (a total of 53 putative pyramidal cells) based upon waveform height, L-ratio, and isolation distance.

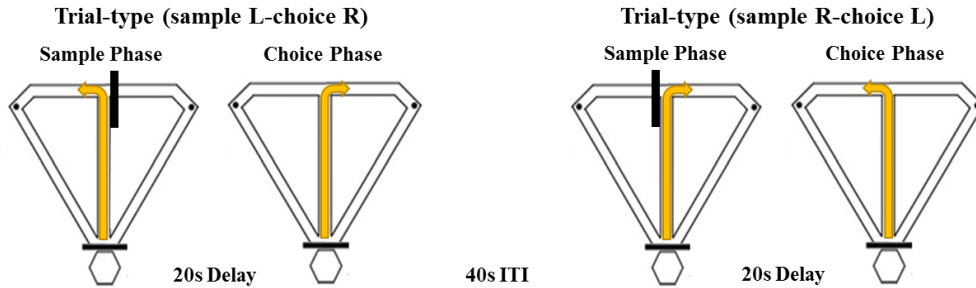


Figure 2: A schematic of the DNMP task. There are two trial-types that are pseudo-randomly selected, one being a sample-left (sample L) traversal followed by a choice-right (choice R) traversal, or a sample-right (sample R) traversal followed by a choice-left (choice L) traversal. Each trial begins with a sample phase where the rat encodes the relevant trajectory and spatial environment while moving down the central stem, to a reward zone and back to the start box via the return arms where the rat is to maintain the previously encoded information for 20 seconds. After the delay, the rat enters the choice phase of the task where the previously encoded information is used to guide a decision at the choice point. If the animal traverses the arm opposite arm to the sample phase, then a rewarded is given. Finally, the rat enters the start-box for a 40 second inter-trial interval which precedes the next trial.

### 3.2 Task Phase-Selective Neurons in the mPFC

Prefrontal units have a variety of firing rate correlates distinct to specific components of SWM tasks; for example, putative pyramidal cells can preferentially fire during the delay, ITI, reward approach, and a combination of task relevant phases (Jung et al., 1998; Yang et al., 2014). Furthermore, it has been demonstrated that mPFC units exhibit different firing rates in the same location in an environment depending on whether the rat is engaged in a hippocampus-dependent DA task or a non-hippocampal dependent visual-tactile CD task (Hallock et al., 2016). Therefore, we first set out to see if we would find task phase-selective units (the firing of a neuron that is specific to the sample or choice phase of the DNMP task – see Figure 2 and methods for information about task phases) in our recordings like has been shown in a population analysis (Spellman et al., 2015). We also wanted to determine if we would see delay-elevated neurons in the mPFC like demonstrated in previous studies (Jung et al., 1998, Yang et al., 2014, Bolkan et al., 2016).

Task phase selectivity was determined for each unit based on whether firing rates differed between the sample and the choice phases, and delay and ITI phases. With this in mind, one unit can exhibit preferential firing for more than one category of task phase selectivity (i.e. a cell that discriminates during the start-box may also show discriminative firing between task phases on the stem) (Figure 3B). A total of 53.3% of all mPFC units recorded were significantly task phase modulated. Of all the units recorded 53.3% were significantly task phase modulated. Specifically, 23.3%

were significantly task phase modulated during the last 5 seconds of start-box occupancy (i.e. showing a change in firing rate during the last 5 seconds of the delay compared to the last 5 seconds of the ITI). 3.3% were significantly task phase modulated by the first 5 seconds of start-box occupancy (task phase modulated between the first 5 seconds of the delay and the first 5 seconds of the ITI). 10% were significantly modulated by task phase during stem traversals (sample phase vs choice phase during stem traversal). Finally, 16.7% were significantly modulated by task phase during choice point occupancy (choice point task phase modulated).

Interestingly, we found that all units that were significantly modulated by late start-box occupancy were located in PL and that 4 out of 7 cells were significantly modulated by the delay (Figure 3C demonstrates a representative unit that fired preferentially for the late delay). These findings support our first prediction that prefrontal units would exhibit delay related activity as has been seen in previous reports (Yang et al., 2014; Spellman et al., 2015; Bolkan et al., 2016). Next, we wanted to determine if the population of cells recorded show start-box and delay-relevant patterns of activity as has been shown previously (Spellman et al., 2015; Hallock et al., 2016; Bolkan et al., 2017; Myroshnychenko et al., 2017).

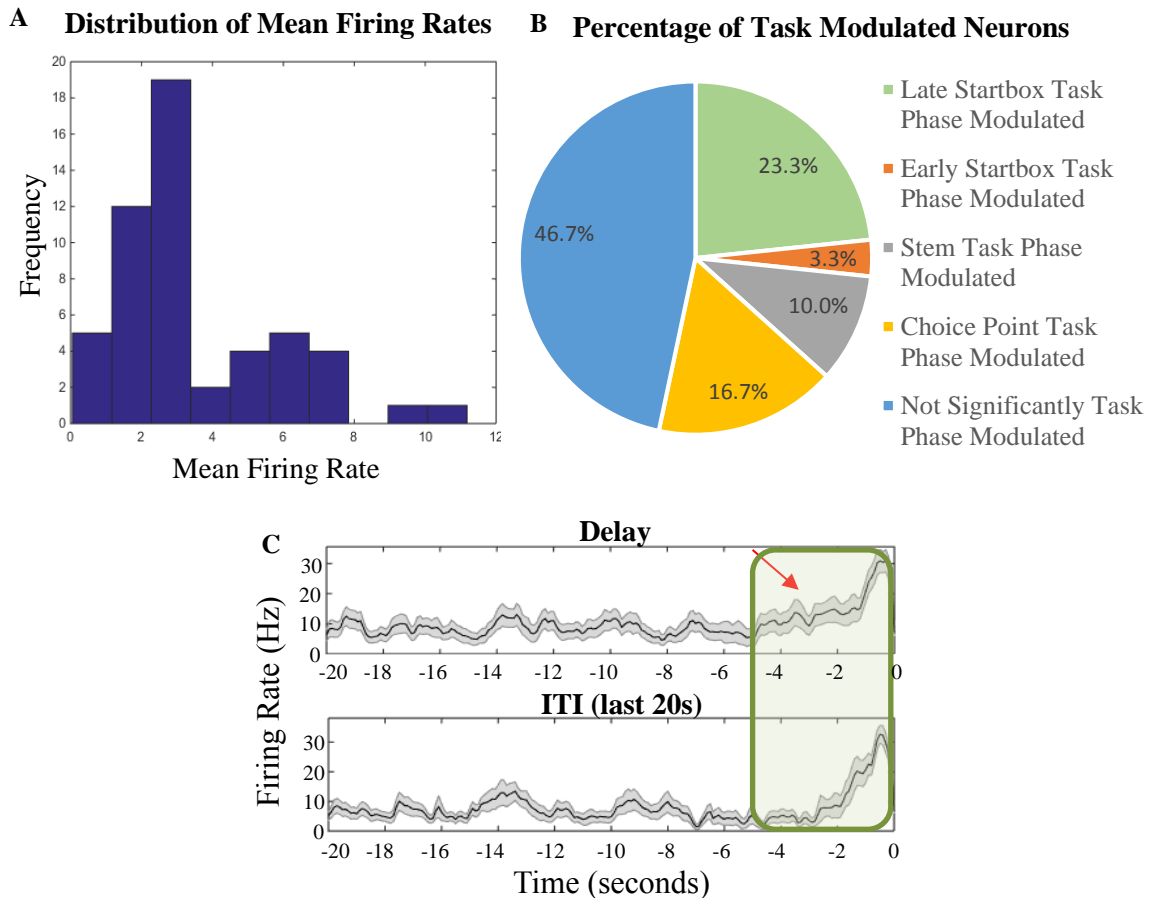


Figure 3: Classification of task modulated prefrontal putative pyramidal cells (N = 53). **A**) Mean firing rate distribution. **B**) Percentages of significantly task modulated units ( $p < 0.05$ , Wilcoxon Signed Rank Test). A total of 53.3% of all mPFC units recorded were significantly task phase modulated. Of all units recorded, 23.3% were significantly task phase modulated by the last 5 seconds of start-box occupancy (late start-box task phase modulated in **green**), 3.3% were significantly task phase modulated by the first 5 seconds of start-box occupancy (early start-box task phase modulated in **orange**), 10% were significantly modulated by task phase during stem traversals (stem task phase modulated in **grey**), and 16.7% were significantly modulated by task phase during choice point occupancy (choice point task phase modulated in **yellow**). **C**) example unit from the last 5 seconds of start-box occupancy – notice the difference in firing rate between the delay and ITI (red arrow).

### **3.3 PL, but Not ACC Population Activity Discriminates Between the Late Portions of the Delay and ITI**

First, we analyzed the entire population of recorded units (mean firing rate distribution can be seen on Figure 3A) and found poor decoding accuracy between delay and ITI at the start-box. To determine whether this poor start-box decoding was due to the fact that we included units from both the ACC and PL, neurons were classified as belonging to PL or ACC (See Figure 1B and methods).

To determine if the PL ensemble distinguishes between the delay and ITI task phases, we trained a linear classifier to distinguish between task-phase using PL and ACC units separately (Figure 4B). PL task phase discrimination between the last 5 seconds of the delay (late delay) and last 5 seconds of the ITI (late ITI) was significantly greater than chance ( $p < 0.01$ , one-sample  $t$ -test) and PL linear classifier percent accuracy was significantly greater than ACC percent accuracy ( $p < 0.01$ , two-sample  $t$ -test). These findings suggest that the PL, but not ACC ensemble is capable of discriminating between the delay and ITI task phases.

A separate, but interesting finding was that classification of task-phase at the bin preceding the choice point is significantly greater than chance level in the ACC population ( $p < 0.001$  one-sample  $t$ -test; Figure 4B). This could be in-line with the role of ACC in motivational states during decision-making (Walton et al., 2002, Walton et al., 2003, Hillman & Bilkey 2010) or reward expectancy neuronal activity (Hyman et al., 2017).

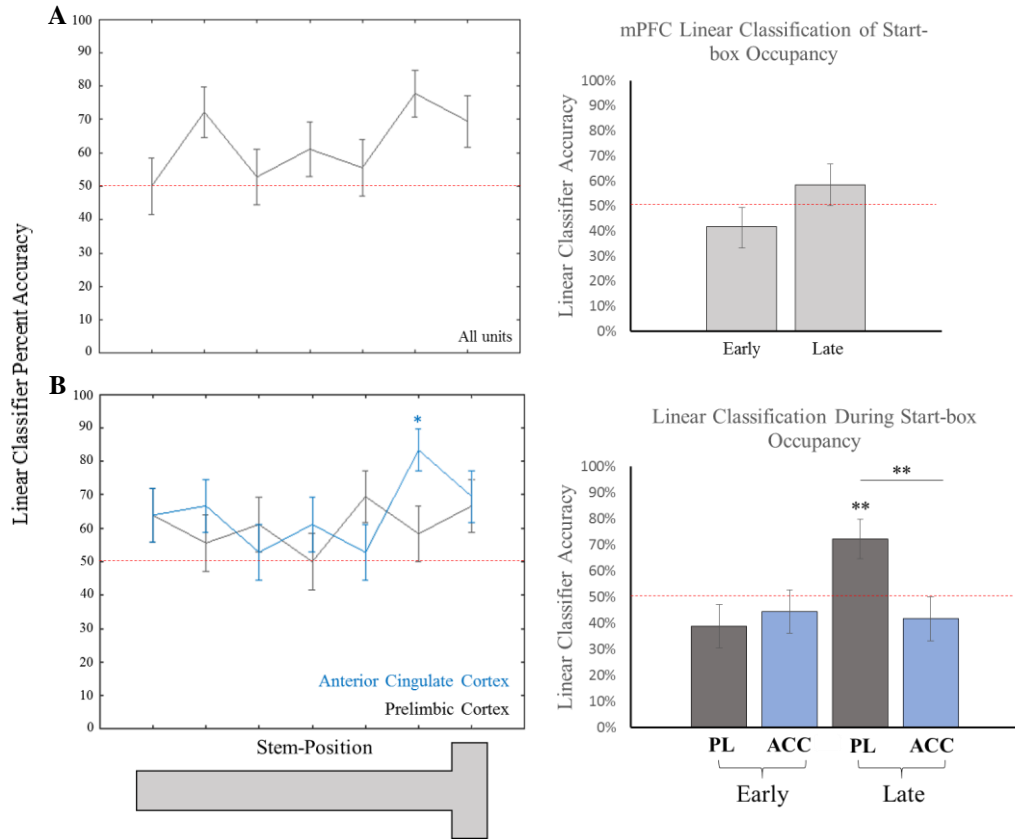


Figure 4: PL, but not ACC population distinguishes between the late delay (last 5 seconds of the delay) and late ITI (last 5 seconds of the ITI). A Linear Classifier was trained to distinguish between task phases (i.e. delay vs ITI, sample stem vs choice stem). The right-most sub-panels for **A** and **B** depicts linear classifier output when trained to distinguish between early delay and ITI (referred to as Early), and trained to distinguish between late delay and ITI (referred to as Late) **A**) Linear classifier trained on all recorded units ( $N = 53$ ) **B**) Linear classifier trained on PL ( $N = 30$ ) and ACC ( $N = 23$ ). PL population activity is predictive of whether the animal is in the late delay or late ITI task phases ( $p < 0.01$  one-sample  $t$ -test) and predicts late start-box occupancy significantly better than ACC ( $p < 0.01$  two-sample  $t$ -test assuming unequal variance) \* indicates  $p < 0.05$ ; \*\* indicates  $p < 0.01$ .

### **3.4 PL Population Activity Distinguishes between Early and Late Start-box Occupancy**

While comparing population firing patterns between the delay and ITI may uncover gross discrimination differences between task-phase, we wanted to determine if there are activity profiles within the delay that could be relevant to SWM. Previous studies have demonstrated that the mPFC population activity exhibits prospective and retrospective coding, or the phenomenon where neurons represent a future or previous experience, respectively (Ito et al., 2015; Myroshnychenko et al., 2017). Therefore, our first prediction was that we would see differential population activity in PL, but not ACC between the early delay (first 5 seconds) and the late delay (last 5 seconds) (see Figure 5A for a depiction of early and late delay). To answer this question, we trained a linear classifier to distinguish between the early and late delay on correct trials. We found that PL but not ACC distinguishes between the early and late delay at a level significantly above chance ( $p < 0.01$  one-sample  $t$ -test) (Figure 5B). This may be in-line with attentional processes or response preparation due to the increase in firing rate observed in the example unit in Figure 5A. Alternatively, these findings could reflect firing rate changes due to a shift from a retrospective to prospective population activity (Myroshnychenko et al., 2017).

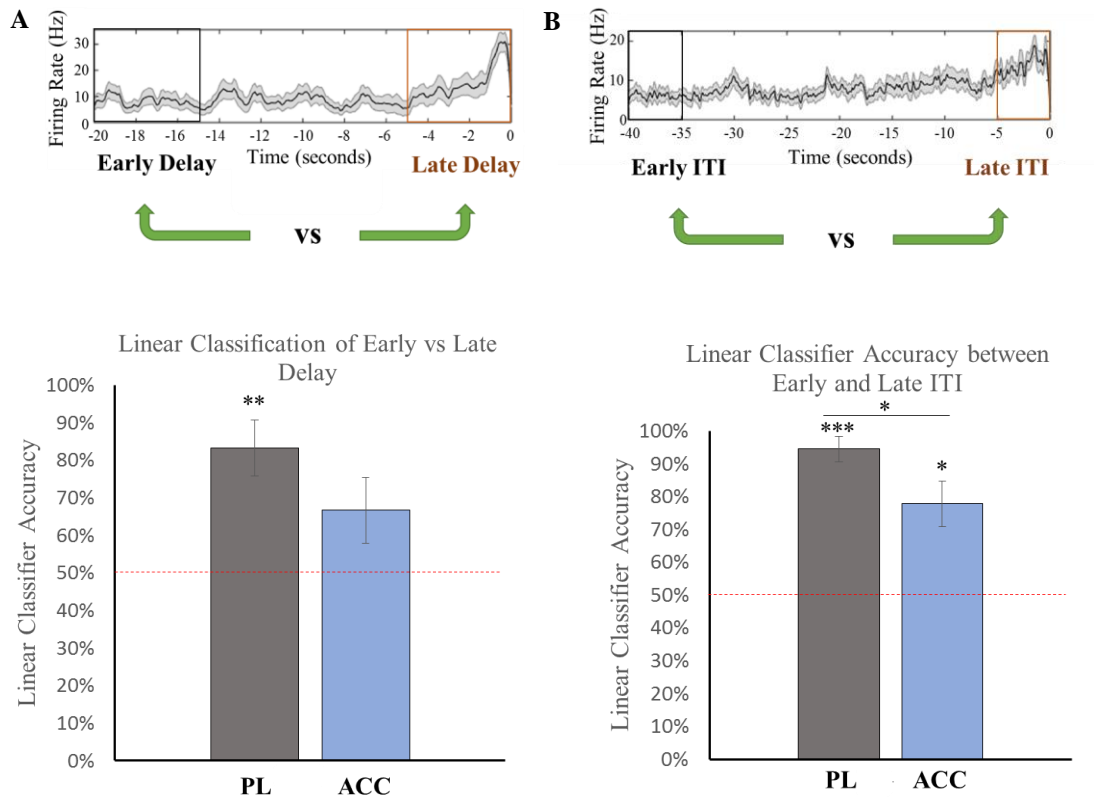


Figure 5: PL distinguishes between early and late start-box occupancy. **A)** Upper panel is an example showing the firing rate of a unit during the delay. Lower panel depicts a linear classifier trained to distinguish between the early and late delay. PL but not ACC population activity distinguishes between the early and late delay at a level significantly above chance (PL  $p < 0.01$  one-sample  $t$ -test; ACC  $p > 0.05$  one-sample  $t$ -test). **B)** Upper panel is an example showing the firing rate of a unit during the ITI. The lower panel depicts a linear classifier trained to distinguish between the early (first 5 seconds) and late (last 5 seconds) ITI. PL distinguishes significantly above chance ( $p < 0.001$  one sample  $t$ -test), ACC distinguishes significantly above chance ( $p < 0.05$  one sample  $t$ -test) and PL better distinguishes between early and late ITI ( $p < 0.05$  two sample  $t$ -test assuming unequal variances). \* indicates  $p < 0.05$ ; \*\* indicates  $p < 0.01$ ; \*\*\* indicates  $p < 0.001$ .

### 3.5 PL Distinguishes Between Distinct Experiences during the Beginning of the Delay

On the DNMP task, there are two kinds of trial-types; trial-types at which the rat turns left at the sample (and right at the choice), and trial-types where the rat turns right at the sample (and left at the choice) (Figure 2, Figure 6A, Figure 7A). Since PL distinguishes between the early and late delay, we next wanted to determine if PL distinguishes between trial-types during the delay. If PL distinguishes between trial-types, it could be possible that PL represents a distinct behavioral context (i.e. a specific trial-type sample phase was just experienced or a specific trial-type choice phase comes next) during the delay instead of only sustaining a representation of a previous or future experience.

To determine if PL population activity distinguishes between trial-types, we first separated the trial-types and isolated the delay period from both. We then trained a linear classifier to distinguish between firing rates from delay periods for trials in which the rat ran left during the sample phase (and will turn right during the choice phase) and trials in which the rat turned right at sample phase (and will turn left during the choice phase). We found that when the entirety of the delay is considered, the population activity does not discriminate between trial-types (Figure 6B). However, when we examined population patterns during the early and late delay, we discovered that the PL population distinguishes between trial-types during the early delay at a level significantly above chance ( $p < 0.05$  one-sample  $t$ -test) and significantly greater than during the late delay ( $p < 0.01$  two-sample  $t$ -test assuming unequal variances)

(Figure 6D and E). These findings suggest that PL is capable of distinguishing between trial-types during the early portion of the delay.

To determine whether our findings were relevant to SWM performance and not due to the animal entering the start-box from two separate return arms, we trained the linear classifier to distinguish between trial-type ITI periods. We found that PL population firing rate patterns distinguish between trial-types during the early delay at a level significantly greater than chance ( $p < 0.05$  one-sample  $t$ -test) (see methods for an explanation on why this was retested), but not significantly greater than chance during the early ITI. We also found that linear classifier accuracy between trial-types during the early delay was significantly greater than that of the early ITI ( $p < 0.001$  two-sample  $t$ -test assuming unequal variances) (Figure 7B and 7C). This finding suggests that PL ensemble distinguishes between two separate experiences that are relevant to SWM.

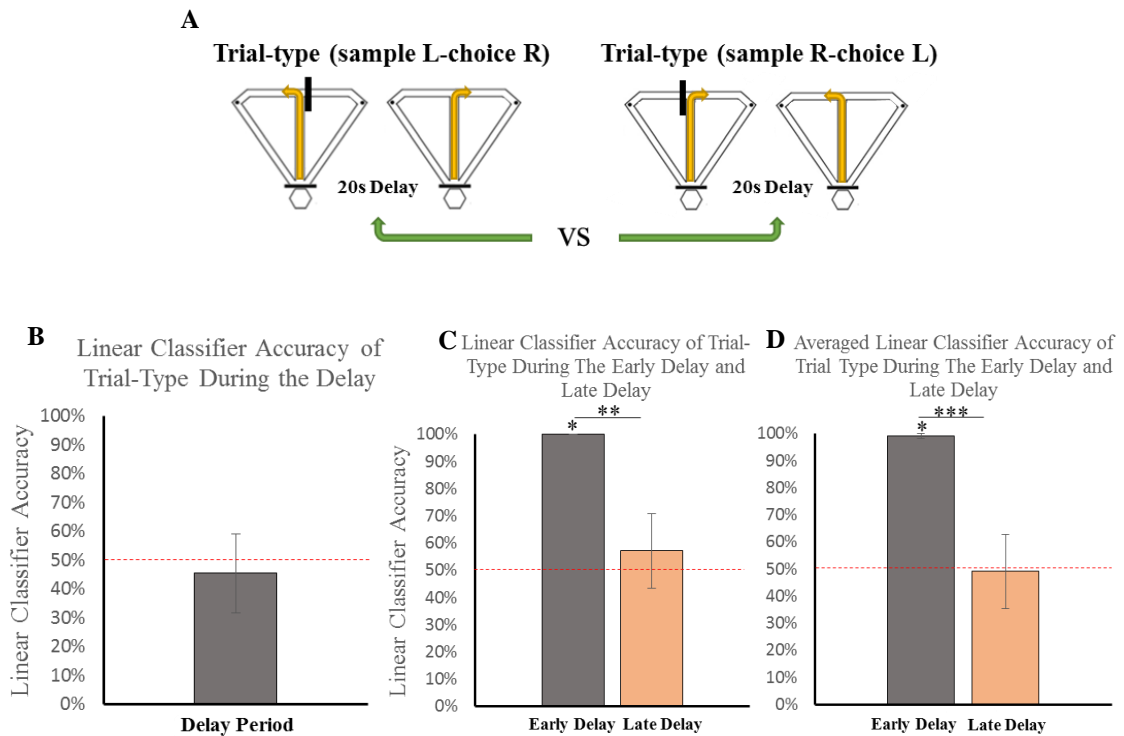


Figure 6: PL population distinguishes between trial-type during early delay. **A)** Depiction of the different trial-types on the DNMP task. **B)** PL population activity ( $N = 30$ ) does not distinguish between trial-types when the classifier is trained on activity during the entire delay ( $p > 0.05$  one-sample  $t$ -test). **C and D)** A linear classifier was trained to distinguish between trial-types during the early and late delay. **C)** Due to an unequal number of trial-types, one trial was randomly removed. PL ensemble can accurately predict the trial-types in the early delay ( $p < 0.05$  one-sample  $t$ -test); prediction is significantly better than during the late delay ( $p < 0.01$  two-sample  $t$ -test assuming unequal variances). **D)** Averaged linear classifier accuracy when each trial was removed separately. PL can accurately distinguish between trial-types during the early delay ( $p < 0.05$  one-sample  $t$ -test) and significantly greater than during the late delay ( $p < 0.001$  two-sample  $t$ -test assuming unequal variances). \* indicates  $p < 0.05$ ; \*\* indicates  $p < 0.01$ ; \*\*\* indicates  $p < 0.001$ .

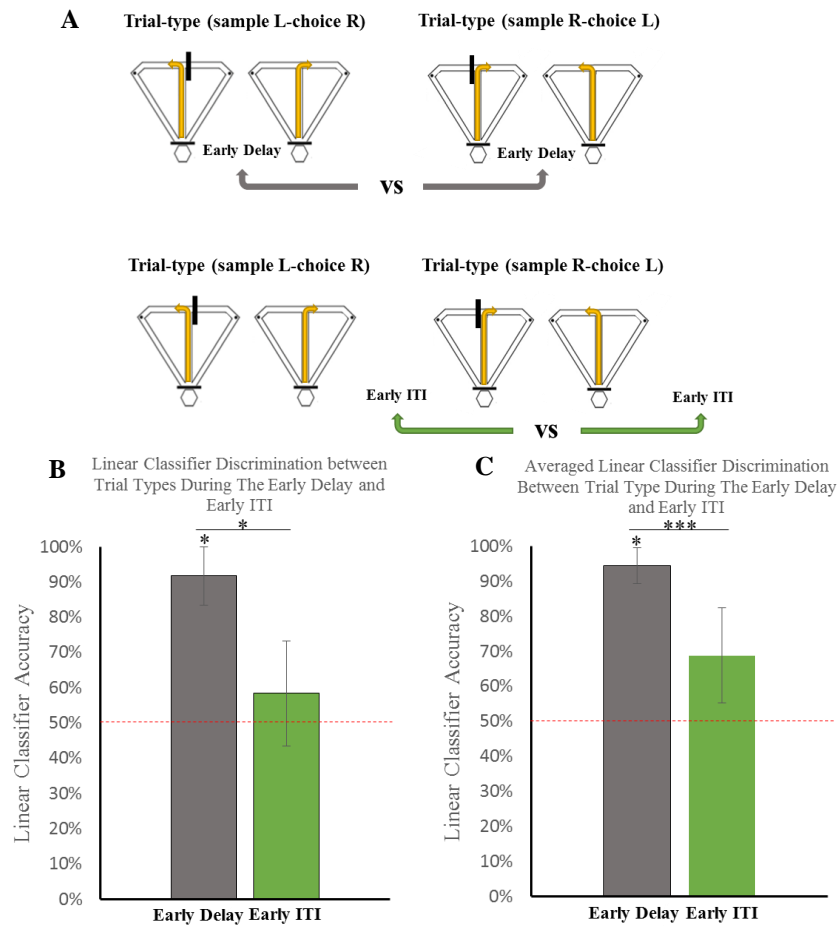


Figure 7: PL distinguishes between trial-type in the early delay, but not significantly above chance during the early ITI. **A)** Schematic of the analysis. **B)** A linear classifier was trained to discriminate between trial-types in the early delay and early ITI. Random deletion of trials within trial-types was utilized due to unequal number of trials between trial-types (see methods). PL distinguishes between trial-types in the early delay significantly greater than chance ( $p < 0.05$  one-sample  $t$ -test) and significantly greater than during the early ITI ( $p < 0.05$  two-sample  $t$ -test assuming unequal variances). PL does not distinguish trial-types significantly above chance during the early ITI ( $p > 0.05$  one-sample  $t$ -test). **C)** Averaged linear classifier percent accuracy. Trials were randomly excluded from the analysis for a total of 12 times (see methods). Linear classifier accuracy is significantly greater in the delay than the ITI ( $p < 0.001$  two-sample  $t$ -test assuming unequal variances), and significantly greater than chance for early delay ( $p < 0.05$  one-sample  $t$ -test), but not for early ITI ( $p > 0.05$  one-sample  $t$ -test). \* indicates  $p < 0.05$ ; \*\*\* indicates  $p < 0.001$ .

## Chapter 4

### DISCUSSION

#### 4.1 A Brief Summary of Our Findings

This study examined the role of the mPFC and two of its sub-regions (ACC and PL) in SWM processes. First, we found that the mPFC exhibits a wide variety of task-correlates, a finding that has been well documented in previous studies (Jung et al., 1998; Yang et al., 2014). Next, we found that ACC neuronal activity discriminates between the encoding and memory-guided decision making task-phases prior to making a decision. This finding could be in-line with reports of the ACC being involved in motivation (Walton et al., 2002; Walton et al., 2003; Hillman & Bilkey 2010) and reward expectancy (Hyman et al., 2017). With respect to PL, we found that PL, but not ACC exhibits high population discrimination between the late, but not early delay and ITI periods. This is supportive of a previous study showing task-phase discrimination towards the end of start-box occupancy in the mPFC of mice (Spellman et al., 2015); however, different because we showed this effect is specific to PL, and also determined that task-coding between the delay and the ITI is selective to late start-box occupancy.

Next, we reported that PL activity both discriminates between the early and late portions of the delay, and early and late portions of the ITI. We propose that this may reflect preparatory processes like preparation to move onto the stem. Finally, we found that PL cortex is capable of distinguishing between two behavioral contexts, or distinct trial-type experiences, during a memory-maintenance period on a DNMP task. While our findings may implicate a retrospective experience, our data differs from previous studies in that we specifically isolated two discrete experiences (trial-types) on the

DNMP task and found firing rate patterns that are distinct for both during the early delay. These findings suggest that PL supports two separate representations for trial-types and we theorize that accessing the relevant representation and monitoring task-phase may be critical to accurate SWM performance. If maintaining the relevant representation during the delay is critical for SWM, these findings may also explain why ACC plays less of a role in the performance of SWM tasks since motivational cues and reward expectancy would follow the maintenance period. Together, our findings suggest that PL cortex integrates behavioral context and task-coding during SWM maintenance.

#### **4.2 Task-Phase Analyses in the mPFC**

As we predicted, we replicated the finding that there is delay-modulated single unit activity, and start-box discriminatory activity (Hallock et al., 2016, Jung et al., 1998; Yang et al., 2014). Utilizing a linear classifier trained on all recorded units, we report poor discrimination between the early portion of the delay and the early portion of the ITI, and poor discrimination between the late portion of the delay and late portion of the ITI. The population in the mPFC (ACC and PL) also discriminates highly before the choice point; however, not significantly above chance (see results).

When we separated ACC and PL, we found sub-regional differences in population activity as expected. Specifically, during late start-box occupancy (last 5 seconds of delay and ITI periods), PL distinguishes between the delay and the ITI significantly above chance and significantly greater than ACC. These findings are supportive of a previous study showing discriminatory differences between task-phase prior to entering the stem in the mPFC (Spellman et al., 2015) but different because we found that PL cortex specifically exhibits task-coding during start-box occupancy,

specifically towards the end of the delay. With respect to the ACC, population discrimination between the sample and choice phase peaks just prior to animals entering the choice point. This could be in line with the ACC's role in motivational states, specifically in determining the cost-benefit outcome of the decision ahead (Walton et al., 2002, Walton et al., 2003, Hillman & Bilkey 2010). To elaborate, if the rat has a bias towards one arm, then a cost-benefit analyses may take place to determine if the reward is worth the effort of traversing the non-preferred arm. To test the involvement of ACC in motivational states on the DNMP task, a future analysis could determine if the animals have a behavioral bias, then separate and examine neuronal activity during left arm traversals and right arm traversals. If the animal exhibits a turn bias, and the activity is reflective of the animals' bias, then our findings may actually represent motivation differences between preferred and non-preferred arms.

Another explanation for ACC activity distinguishing between task phase at the choice-point could be related to its role in reward expectancy signaling (Hyman et al., 2017). To elaborate, since the animals receive a reward following a decision, it would be beneficial for the animal to predict whether their actions will yield this reward. A future analysis will examine error trials to determine if ACC activity prior to making a choice is linked with accurate decision-making on the DNMP task. Interestingly, since ACC lesions do not result in SWM impairments (Ragozzino et al., 1998), it could be possible that the ACC is more critically involved in learning the DNMP task. Future experiments could inactivate the ACC during the learning process to gauge its involvement and determine if the pairing of expectancy related signals with a choice is critical to the learning of SWM tasks.

### **4.3 PL Cortex Exhibits Differential Activity Between the Beginning and End of Start-box Occupancy**

We have reported that PL, but not ACC population activity is capable of distinguishing between the early (first 5 seconds) and late (last 5 seconds) epochs of the delay period at a level significantly above chance. Interestingly, PL population firing rates also differentiate between the early and late ITI. These findings may reflect a general phenomenon whereby neuronal activity between the beginning and the end of start-box occupancy is different. Future analyses will examine the directionality of change in firing rates between the beginning and the end of start-box occupancy. It's possible that PL units exhibit elevated activity prior to entering the stem, reflecting a preparation for the animal to move, or reflecting the barrier to the stem being lifted by the experimenter.

### **4.4 Prelimbic Population Activity Distinguishes Between Distinct Experiences**

Previous work has demonstrated that PL cortex is capable of shifting its representation from most closely matching an encoding phase, to most closely matching a memory-guided decision-making phase (Myroshnychenko et al., 2017). Instead of examining whether activity in the delay generally represents an encoding or retrieval phase only, we wanted to determine if the PL firing rate patterns distinguish between two spatially-distinct experiences on the DNMP task and if this activity is relevant to SWM. Therefore, we predicted that we would see firing rate population differences during the delay period that were contingent upon trial-type (sample L-choice R vs sample R-choice L). We report that during the entirety of the delay, there are no observed population discrimination patterns that distinguish trial-type. However, when we examined the early and late portions of the delay, we observed that the PL cortex distinguishes between trial-types with high accuracy specifically in the

early delay, and not in the late delay. This suggests that during the early portion of the delay, PL units represent a distinct behavioral context. However, to determine if these findings were relevant for SWM and not reflective of the most recent trajectory, we trained a linear classifier to distinguish between trial-types during the early ITI. We found that PL does not distinguish between trial-types significantly above chance during the early ITI and that PL distinguishes between trial-types significantly better during the early delay. Therefore, these findings suggest that during early SWM maintenance following a recent goal-relevant encoding experience, PL activity may represent distinct experiences, distinct rules related to the DNMP task, or distinct encoding/retrieval phases of SWM. We define this phenomenon as behavioral context and propose that PL distinguishes between behavioral contexts during early SWM maintenance. Future work could further determine if these findings are necessary for SWM by examining neuronal population activity during poor performance sessions and comparing the findings with those presented in this thesis.

A limitation to this study is that our analyses were run using a small sample size of cells. Future work is aimed at recording more ACC and PL neurons to determine if this phenomenon is conserved across a larger population.

#### **4.5 Conclusion**

The findings in this thesis support the growing body of literature on the role of PL cortex in SWM maintenance processes and ACC in decision-making. Specifically, our findings implicate that the PL cortex integrates behavioral context with task-coding during the maintenance-period of SWM, while ACC grossly distinguishes between task-phases prior to making a decision. While a previous report has shown task-phase differences between the delay and ITI in the mPFC prior to entering the

stem (Spellman et al., 2015), we have reported that this phenomenon seems to specifically exist in the PL cortex of the rat. We also report that this task-coding between the delay and ITI does not exist during the beginning of the delay. Next we showed that PL cortex population activity differentiates between the early and late delay, and the early and late ITI periods, possibly reflecting preparatory processes. Furthermore, while PL cortex during the early delay is reflective of a previous experience on a separate SWM task (Myroshnychenko et al., 2017), we suggest that PL cortex also distinguishes between behavioral contexts and that two separate representations exist between trial-types during early SWM maintenance. In summary, our findings contribute to the ACC literature by demonstrating that ACC distinguishes between task-phases prior to making a decision as rats perform a DNMP task. Furthermore, we report that PL cortex plays a role in distinguishing between behavioral contexts in the beginning of the delay and task-coding towards the end portraying that the PL cortex integrates behavioral context and task-coding during the maintenance of spatial working memories.

## REFERENCES

- Baeg, E. H., Kim, Y. B., Huh, K., Mook-Jung, I., Kim, H. T., & Jung, M. W. (2003). Dynamics of population code for working memory in the prefrontal cortex. *Neuron*, *40*(1), 177-188.
- Bolkan, S. S., Stujenske, J. M., Parnaudeau, S., Spellman, T. J., Rauffenbart, C., Abbas, A. I., ... & Kellendonk, C. (2017). Thalamic projections sustain prefrontal activity during working memory maintenance. *Nature neuroscience*, *20*(7), 987.
- Brown, V. J., & Bowman, E. M. (2002). Rodent models of prefrontal cortical function. *Trends in neurosciences*, *25*(7), 340-343.
- Churchwell, J. C., & Kesner, R. P. (2011). Hippocampal-prefrontal dynamics in spatial working memory: interactions and independent parallel processing. *Behavioural brain research*, *225*(2), 389-395.
- Cook, R. G., Brown, M. F., & Riley, D. A. (1985). Flexible memory processing by rats: Use of prospective and retrospective information in the radial maze. *Journal of Experimental Psychology: Animal Behavior Processes*, *11*(3), 453.
- Floresco, S. B., Seamans, J. K., & Phillips, A. G. (1997). Selective roles for hippocampal, prefrontal cortical, and ventral striatal circuits in radial-arm maze tasks with or without a delay. *Journal of Neuroscience*, *17*(5), 1880-1890.
- Fuster, J. M., & Alexander, G. E. (1971). Neuron activity related to short-term memory. *Science*, *173*(3997), 652-654.

- Goldman-Rakic, P. S. (1995). Cellular basis of working memory. *Neuron*, 14(3), 477-485.
- Griffin, A. L., Eichenbaum, H., & Hasselmo, M. E. (2007). Spatial representations of hippocampal CA1 neurons are modulated by behavioral context in a hippocampus-dependent memory task. *Journal of Neuroscience*, 27(9), 2416-2423.
- Hallock, H. L., Wang, A., & Griffin, A. L. (2016). Ventral midline thalamus is critical for hippocampal–prefrontal synchrony and spatial working memory. *Journal of Neuroscience*, 36(32), 8372-8389.
- Hillman, K. L., & Bilkey, D. K. (2010). Neurons in the rat anterior cingulate cortex dynamically encode cost–benefit in a spatial decision-making task. *Journal of Neuroscience*, 30(22), 7705-7713.
- Hyman, J. M., Holroyd, C. B., & Seamans, J. K. (2017). A novel neural prediction error found in anterior cingulate cortex ensembles. *Neuron*, 95(2), 447-456.
- Ito, H. T., Zhang, S. J., Witter, M. P., Moser, E. I., & Moser, M. B. (2015). A prefrontal–thalamo–hippocampal circuit for goal-directed spatial navigation. *Nature*, 522(7554), 50.
- Jung, M. W., Qin, Y., McNaughton, B. L., & Barnes, C. A. (1998). Firing characteristics of deep layer neurons in prefrontal cortex in rats performing spatial working memory tasks. *Cerebral cortex (New York, NY: 1991)*, 8(5), 437-450.

- Kesner, R. P. (1989). Retrospective and prospective coding of information: role of the medial prefrontal cortex. *Experimental Brain Research*, 74(1), 163-167.
- Kesner, R. P. (2000). Subregional analysis of mnemonic functions of the prefrontal cortex in the rat. *Psychobiology*, 28(2), 219-228.
- Kesner, R. P., & Churchwell, J. C. (2011). An analysis of rat prefrontal cortex in mediating executive function. *Neurobiology of learning and memory*, 96(3), 417-431.
- Lee, I., & Kesner, R. P. (2003). Time-dependent relationship between the dorsal hippocampus and the prefrontal cortex in spatial memory. *Journal of Neuroscience*, 23(4), 1517-1523.
- Myroshnychenko, M., Seamans, J. K., Phillips, A. G., & Lapish, C. C. (2017). Temporal Dynamics of Hippocampal and Medial Prefrontal Cortex Interactions During the Delay Period of a Working Memory-Guided Foraging Task. *Cerebral Cortex*, 27(11), 5331-5342.
- Neave, N., Lloyd, S., Sahgal, A., & Aggleton, J. P. (1994). Lack of effect of lesions in the anterior cingulate cortex and retrosplenial cortex on certain tests of spatial memory in the rat. *Behavioural brain research*, 65(1), 89-101.
- Paxinos, G., and C. Watson. "The rat brain atlas." *San Diego, CA: Academic* (1986).
- Ragozzino, M. E., Adams, S., & Kesner, R. P. (1998). Differential involvement of the dorsal anterior cingulate and prelimbic–infralimbic areas of the rodent prefrontal cortex in spatial working memory. *Behavioral neuroscience*, 112(2), 293.

- Sánchez-Santed, F., de Bruin, J. P., Heinsbroek, R. P., & Verwer, R. W. (1997). Spatial delayed alternation of rats in a T-maze: effects of neurotoxic lesions of the medial prefrontal cortex and of T-maze rotations. *Behavioural Brain Research*, 84(1), 73-79.
- Schmitt, L. I., Wimmer, R. D., Nakajima, M., Happ, M., Mofakham, S., & Halassa, M. M. (2017). Thalamic amplification of cortical connectivity sustains attentional control. *Nature*, 545(7653), 219-223.
- Schmitzer-Torbert, N., Jackson, J., Henze, D., Harris, K., & Redish, A. D. (2005). Quantitative measures of cluster quality for use in extracellular recordings. *Neuroscience*, 131(1), 1-11.
- Spellman, T., Rigotti, M., Ahmari, S. E., Fusi, S., Gogos, J. A., & Gordon, J. A. (2015). Hippocampal–prefrontal input supports spatial encoding in working memory. *Nature*, 522(7556), 309.
- Walton, M. E., Bannerman, D. M., & Rushworth, M. F. (2002). The role of rat medial frontal cortex in effort-based decision making. *Journal of Neuroscience*, 22(24), 10996-11003.
- Walton, M. E., Bannerman, D. M., Alterescu, K., & Rushworth, M. F. (2003). Functional specialization within medial frontal cortex of the anterior cingulate for evaluating effort-related decisions. *Journal of Neuroscience*, 23(16), 6475-6479.

Wang, G. W., & Cai, J. X. (2006). Disconnection of the hippocampal–prefrontal cortical circuits impairs spatial working memory performance in rats. *Behavioural brain research*, 175(2), 329-336.

Yang, S. T., Shi, Y., Wang, Q., Peng, J. Y., & Li, B. M. (2014). Neuronal representation of working memory in the medial prefrontal cortex of rats. *Molecular brain*, 7(1), 61

## Appendix A

### ANIMAL PROTOCOL PERMISSION



Institutional Animal Care  
and Use Committee (IACUC)

Newark, DE 19716-1561  
Phone: 302-831-2616  
Fax: 302-831-0154  
Email: [iam-iacuc@udel.edu](mailto:iam-iacuc@udel.edu)

To: Office of Graduate and Professional Education

From: Gwen Talham, DVM, Director, Animal Care Program

A handwritten signature in purple ink, appearing to be 'GWT', written over the 'From:' line.

Subject: IACUC approval for John Stout

Date: 4/2/2018

John Stout was approved by the IACUC to work with animals on Amy Griffin's protocol #1177 "Neural Correlates of Spatial and Nonspatial Memory". Please contact me at 831-2980 or [gtalham@udel.edu](mailto:gtalham@udel.edu) with any additional questions.